ZOOLOGICAL RESEARCH

A soluble FcγR homolog inhibits IgM antibody production in ayu spleen cells

Kai Chen[1], Yu-Hong Shi[1,2,*], Jiong Chen[1,2,*], Ming-Yun Li[1]

[1] *Laboratory of Biochemistry and Molecular Biology*, *School of Marine Sciences*, *Ningbo University*, *Ningbo Zhejiang* 315832, *China*

[2] *State Key Laboratory for Quality and Safety of Agro-products*, *Ningbo University*, *Ningbo Zhejiang* 315211, *China*

ABSTRACT

Classical Fc receptors (FcRs) mediate the binding to and recognition of the Fc portion of antibodies and play an important role during immune responses in mammals. Although proteins similar to soluble FcRs have been identified in fish, little is known about the role of such proteins in fish immunity. Here, we cloned a cDNA sequence encoding a soluble Fc receptor for an immunoglobulin G (FcγR) homolog from ayu (*Plecoglossus altivelis*) (PaFcγRl). The predicted protein was composed of two immunoglobulin C2-like domains but lacked a transmembrane segment and a cytoplasmic tail. The PaFcγRl transcripts were distributed at low levels in all tested tissues, but significantly increased after *Vibrio anguillarum* infection. The PaFcγRl protein was expressed in the head kidney, trunk kidney, and neutrophils. Recombinant PaFcγRl (rPaFcγRl) was secreted when transfected into mammalian cells and the native protein was also detected in serum upon infection. rPaFcγRl was also demonstrated to bind to ayu IgM, as assessed by cell transfection. Suppressive activity of the recombinant mature protein of PaFcγRl (rPaFcγRlm) on *in vitro* anti-sheep red blood cell (SRBC) responses was detected by a modified hemolytic plaque forming cell assay. In conclusion, our study revealed that PaFcγRl is closely involved in the negative regulation of IgM production in the ayu spleen.

Keywords: Soluble FcγR homolog; Sequence characterization; IgM-binding protein; Inhibition of IgM production; *Plecoglossus altivelis*

INTRODUCTION

Antibodies are key components of the immune system, linking both innate and adaptive immunity (Bournazos & Ravetch, 2015). The variable Fab region of an antibody mediates specificity and dictates to what antigen and with what affinity the antibody will bind to its target. Antibodies also contain a constant region, termed the Fc domain, which engages diverse cellular receptors, thereby triggering antibody-mediated effector functions in innate and adaptive immunity (Dilillo & Ravetch, 2015). As members of the immunoglobulin (Ig) superfamily, Fc receptors (FcRs) are broadly expressed on the surface of various myeloid leukocytes and mediate binding and recognition of the Fc portion of antibodies (Davis, 2007). Since their identification three decades ago, our understanding of the biological consequences of FcRs has continued to evolve. FcRs mediate various functions including phagocytosis, antibody-dependent cell-mediated cytotoxicity, lymphocyte proliferation, mast cell degranulation, release/secretion of cytokines and chemokines, antigen presentation,

Received: 18 February 2019; Accepted: 26 June 2019; Online: 23 July 2019

Foundation items: This project was supported by the Program for the National Natural Science Foundation of China (31772876; 31402323; 31372555), Natural Science Foundation of Zhejiang Province (LZ18C190001; LY14C190007), Scientific Innovation Team Project of Ningbo (2015C110018), Natural Science Foundation of Ningbo City of China (2018A610225), Ningbo Science and Technology "Fumin Engineering" Project (2017C10037), and K. C. Wong Magna Fund in Ningbo University

*Corresponding authors, E-mail: shiyuhong0517@163.com; jchen1975@163.com

DOI: 10.24272/j.issn.2095-8137.2019.056

regulation of antibody production, clearance of immune complexes, and Ig transport (Bournazos & Ravetch, 2015; Nayak et al., 2010).

Mammals express six different Ig classes: i. e., IgG, IgM, IgD, IgE, IgA, and IgO. Correspondingly, four major classical FcRs have been identified for IgG (FcγRI, FcγRII, FcγRIII, and FcγRIV), as well as one for IgE (FcεRI), one for both IgM and IgA (FcαμR), one for IgM (FcμR), and one for IgA (FcαRI) in most previously studied placental mammals (Akula et al., 2014). The α chains of these receptors, which are Ig-binding subunits, are all related in structure, thus suggesting an origin from one or a few common early ancestors via successive gene duplications (Davis et al., 2005). In most instances, classical mammalian FcR genes consist of extracellular C2 Ig domains as well as a transmembrane (TM) segment and a cytoplasmic tail (CYT), which may contain signaling motifs (Stafford et al., 2006).

Soluble forms of FcRs (sFcRs) have been identified in the sera and supernatants of activated cells, including T cells, B cells, fibroblasts, macrophages, NK cells, and Langerhans cells (Esposito-Farese et al., 1995). sFcRs are produced either by cleavage at the cell membrane or by secretion of molecules generated by splicing of the TM-encoding exon. Soluble forms exist in the extracellular portion of the receptor or extracellular region linked to the intracytoplasmic portion of the receptor (Rosales & Uribe-Querol, 2013). sFcRs have been described for FcγRI, FcγRII, FcγRIII, FcεRII, and FcαRI (Daëron et al., 1989; Matt et al., 2015; Sarfati et al., 1996; van der Boog et al., 2002). Among these sFcRs, soluble FcγRs (sFcγRs) are relatively well studied and shown to play a regulatory role in immune responses. For example, sFcγRs bind to the Fc domains of IgG to exert immunoregulatory activities *in vivo* and *in vitro*, including the inhibition of IgG and IgM antibody production (Fridman et al., 1992) and immune complex precipitation (Gavin et al., 1995). In addition, sFcγRs are also reported to function in the inhibition of C1q binding and complement activation, antibody dependent cellular cytotoxicity, and antigen-antibody uptake (Molenaar et al., 1977).

To date, four classes of Ig have been reported in teleosts, including IgM, IgD, IgZ/IgT, and IgM−IgZ chimera, with IgM reported first (Tian et al., 2009). Of the classical Ig-binding FcR homologs, however, only FcεRIγ has been identified in teleosts, which has limited our understanding not only of the evolutionary history of FcRs but also their functional significance in ectotherms (Akula et al., 2014). Interestingly, FcR homologs without a TM or CYT have been identified in teleosts by genomic/transcriptomic analysis, with the first reported in channel catfish (*Ictalurus punctatus*) (i. e., IpFcRI) (Stafford et al., 2006). IpFcRI is structurally conserved, containing extracellular domains, as found in classical FcRs, and maintaining three Ig domains and Fc-binding sites for antibody recognition (Stafford et al., 2006). Furthermore, IpFcRI binds to IgM as a soluble protein in serum (Nayak et al., 2010; Stafford et al., 2006). Such proteins are also found in many other bony fish, e.g., zebrafish (*Danio rerio*), rainbow trout (*Oncorhynchus mykiss*), tiger puffer (*Takifugu rubripes*), and spotted green pufferfish (*Tetraodon nigroviridis*) (Akula et al., 2014; Stafford et al., 2006). To date, however, little is known about the function of these receptors.

Ayu (*Plecoglossus altivelis*) is an economically important fish in East Asia (Nishimori et al., 2000). Recently, however, the development of ayu aquaculture in China has been severely challenged by *Vibrio anguillarum* infection, which has resulted in both production and animal welfare problems (Li et al., 2009; Nishimori et al., 2000; Xiong et al., 2018). Given the importance of FcRs in innate immunity, understanding the function and mechanism of action of ayu FcRs would be helpful for disease control and prevention. In this study, a novel sFcγR-like gene (PaFcγRI) was identified from ayu. The mRNA expression profiles of PaFcγRI in healthy and *V. anguillarum*-infected tissues were determined. The IgM-binding activity of PaFcγRI and its effect on IgM antibody production in spleen cells were also preliminarily characterized.

MATERIALS AND METHODS

Molecular characterization of PaFcγRI

The cDNA sequence of PaFcγRI was obtained from transcriptome data of ayu head kidney-derived monocytes/macrophages (MO/MΦ) using a BLAST search (http://blast.ncbi.nlm.nih.gov/Blast.cgi). The sequence was then used to design primers for specific amplification of the objective gene sequence from cDNA, with the amplicons sequenced on an ABI 3730 automated sequencer (Invitrogen, Shanghai, China) to confirm the correctness of the PaFcγRI sequence. SignalP v4.1 (http://www.cbs.dtu.dk/services/SignalP/) was used to predict the cleavage sites of the signal peptides. The molecular weights (MW) and isoelectric points (*p*I) were predicted using the Compute *p*I/Mw tool (http://web.expasy.org/compute_pi/). The N-glycosylation sites were predicted using the NetNGlyc 1.0 server (http://www.cbs.dtu.dk/services/NetNGlyc/). The SMART program (http://smart.embl-heidelberg.de/) was used to predict the domain architecture of the putative protein. Multiple sequence alignment was analyzed using ClustalW (http://clustalw.ddbj.nig.ac.jp/), and phylogenetic analyses were conducted using MEGA v7.0 (Kumar et al., 2016). Sequences used in this study are listed in Table 1.

Fish and *V. anguillarum* infection challenge

Healthy fish weighing 50−60 g each were purchased from a commercial farm in Ninghai County, China, and maintained in 100 L tanks at 20−22 °C with regular feeding, as described previously (Chen et al., 2016). The fish were acclimatized to laboratory conditions for two weeks before experiments were conducted. All experiments were performed according to the Experimental Animal Management Law of China and approved by the Animal Ethics Committee of Ningbo University.

The *V. anguillarum* artificial infection experiment was carried out as reported previously (Chen et al., 2016). Briefly, bacteria were grown in nutrient broth on a rotary shaker at 28 °C and

Table 1 Sequences of FcγR used in the study

GenBank accession No.	Species		Protein
	Latin name	English name	
XM022404314	*Canis lupus familiaris*	Dog	FcγRI
L03418	*Homo sapiens*	Human	FcγRI
EU589389	*Ovis aries*	Sheep	FcγRII
NM001136219	*H. sapiens*	Human	FcγRIIA
NM001002274	*H. sapiens*	Human	FcγRIIB
DQ026064	*Sus scrofa*	Pig	FcγRIIB
NM201563	*H. sapiens*	Human	FcγRIIC
NM010188	*Mus musculus*	Mouse	FcγRIII
EU589390	*O. aries*	Sheep	FcγRIII
AF132036	*Bos taurus*	Cow	FcγRIII
NM001127596	*H. sapiens*	Human	FcγRIII
BC027310	*M. musculus*	Mouse	FcγRIV
NM004106	*H. sapiens*	Human	FcεRγ
XM018231525	*Xenopus laevis*	African clawed frog	FcRL5
XM018096520	*Xenopus tropicalis*	Tropical clawed frog	FcRL5
NM001184866	*H. sapiens*	Human	FcRLA
MG687271	*Plecoglossus altivelis*	Ayu	FcγRI
XM019102455	*Cyprinus carpio*	Common carp	FcεRαL
XM011608346	*Takifugu rubripes*	Tiger pufferfish	FcεRα
XM021478104	*Danio rerio*	Zebrafish	FcRL5
XM012871848	*Fundulus heteroclitus*	Mummichog	FcRLA
XM014331816	*Haplochromis burtoni*	African cichlid fish	FcRLA
CAF97406	*Tetraodon nigroviridis*	Spotted green pufferfish	FcR
DQ286290	*Ictalurus punctatus*	Channel catfish	FcRI
XM010738182	*Larimichthys crocea*	Large yellow croaker	FcRLA
XM018702142	*Lates calcarifer*	Asian seabass	FcγRIL
XM020503104	*Oncorhynchus kisutch*	Coho salmon	FcγRIL
XM021587750	*Oncorhynchus mykiss*	Rainbow trout	FcγRIL
XM019367764	*Oreochromis niloticus*	Nile tilapia	FcγRIIIA
XM011482503	*Oryzias latipes*	Japanese ricefish	FcγRIVL
XM015041400	*Poecilia latipinna*	Sailfin molly	FcRL4
XM014162558	*Salmo salar*	Atlantic salmon	FcγRIL
XM020928651	*Boleophthalmus pectinirostris*	Mudskipper	FcγRIVL

harvested in the logarithmic phase of growth, as monitored by optical density assay. The *V. anguillarum* cells were washed, resuspended, and diluted to an appropriate concentration in sterile phosphate buffer saline (PBS). Fish were challenged by intraperitoneal injection with 1.2×10^4 colony forming units (CFUs) of live *V. anguillarum* (in 100 μL PBS) per fish, with PBS alone used as the control. At 4, 8, 12, and 24 h post-infection (hpi), tissue samples were collected and immediately snap-frozen in liquid nitrogen. Blood samples were allowed to clot overnight, after which serum was collected by centrifugation at 13 000 r/min for 15 min at 4 °C. All tissues and sera were preserved at −80 °C until subsequent use.

Real-time quantitative polymerase chain reaction (RT-qPCR)

Total RNA extraction, first strand cDNA synthesis, and RT-qPCR were carried out as reported previously (Ren et al., 2019). The tPaFcγRI(+) and tPaFcγRI(−) primers were used to produce a 227 bp fragment ("t" in the primer name stands for "test") (Table 2). The Pa18S rRNA(+) and Pa18S rRNA(−) primers were used to produce a 116 bp fragment of the housekeeping 18S rRNA gene, which is widely used as an internal control (Table 2). The RT-qPCR protocol was: 94 °C for 5 min, 40 cycles of 94 °C for 30 s, 60 °C for 30 s, and 72 °C for 30 s in a RT-Cycler™ real-time fluorescence quantitative

PCR thermocycler (CapitalBio, Beijing, China). The mRNA expression of PaFcγRI was normalized against that of 18S rRNA, and the quantitative differences between expression levels were calculated using the $2^{-\Delta\Delta Ct}$ method in the *V. anguillarum* infection challenge assay (Livak & Schmittgen, 2001). All data were analyzed by one-way analysis of variance (ANOVA) with SPSS (v13.0, Chicago, IL, USA). $P<0.05$ was considered statistically significant.

Table 2 Primers used in the study

Primer	Gene	GenBank accession No.	Nucleotide sequence (5′–3′)	Length (bp)
tPaFcRI(+)	PaFcγRI	MG687271	CAGAGCAGCAGAGTCACAGC	227
tPaFcRI(−)			TGGGGACGAAGATTGAGTTC	
Pa18S rRNA (+)	Pa18S rRNA	FN646593	GAATGTCTGCCCTATCAACT	116
Pa18S rRNA (−)			GATGTGGTAGCCGTTTCT	
rPaFcγRI(+)	PaFcγRI	MG687271	CAAGCTTATGTTCACTGTATGTTGTGAC[a]	926
rPaFcγRI(−)			TTGCGGCCGCCTACACAGTGGTGATCTCAC[b]	
rPaFcγRIm (+)	PaFcγRI	MG687271	GGGAATTCAGACCTTCTGGCTGAAGTCC[c]	810
rPaFcγRIm (−)			CCTCGAGCTACACAGTGGTGATCTCAC[d]	
rPaIgM-Fc(+)	PaIgM-Fc	AB703441	GGAATTCAATAAGACGGCTTCCTTCG C[c]	1011
rPaIgM-Fc (−)			CCTCGAGCTACTGGGCTATGCAGGAGG[d]	
TM-PaIgM-P1(+)	PaCTLRC	KP329196	CGGGATCCCAGGGGGGTCAGGGGCCCTA[e]	111
TM-PaIgM-P1(−)			CAGGCTCCTGTAGCGGGCAC	
TM-PaIgM-P2(+)	PaIgM	AB703441	GTGCCCGCTACAGGAGCCTGATGTTCTCTGTTTCGCTGCT	1761
TM-PaIgM-P2(−)			CGGAATTCCTACTGGGCTATGCAGGAG[a]	
TM-P1(+)	PaCTLRC	KP329196	CGGGATCCCAGGGGGGTCAGGGGCCCTA[e]	117
TM-P1(−)			CGGAATTCCTACAGGCTCCTGTAGCGGGCAC[a]	

[a, b, c, d] and [e]: Underlined regions indicate restriction enzyme sites *Hind* III, *Not* I, *Eco*R I, *Xho* I, and *Bam*H I, respectively.

Prokaryotic expression and purification of recombinant proteins

In this study, the recombinant mature proteins of PaFcγRI (rPaFcγRIm) and the Fc portion of the ayu IgM (rPaIgM-Fc) were prokaryotically expressed. The primers for amplification of the two genes are listed in Table 2. The prokaryotic expression and purification have been described previously (Zhang et al., 2011). Briefly, amplicons of expected size were digested by *Eco*R I and *Xho* I, and subsequently inserted into the pET30a(+) vector. The recombinant plasmids were then transformed into *Escherichia coli* BL21 (DE3) for overexpression. After overexpression was identified by SDS-PAGE analysis, the isopropyl β-D-thiogalactoside (IPTG)-induced cultures were harvested, and the cell pellets were resuspended in 20 mL of sonication buffer. After sonication, the inclusion bodies were recovered and resuspended in 2 mL of buffer A (0.1 mol/L Tris-HCl, 0.5 mol/L NaCl, 10 mmol/L imidazole, and 8 mol/L urea, pH 7.5). The purification of solubilized recombinant proteins was performed on a HisTrap™ FF (GE Healthcare, Shanghai, China) and gradient eluted with buffer B (0.1 mol/L Tris-HCl, 0.5 mol/L NaCl, 500 mmol/L Imidazole and 8 mol/L urea, pH 7.5) increasing from 0 to 100%. The peak fractions were pooled and dialyzed with solubilization buffer (50 mmol/L KH_2PO_4, 1 mmol/L EDTA, and 300 mmol/L KCl, containing 8 mol/L urea and 0.2 mol/L DTT, pH 8.0) and then concentrated using a 10 000 NMWL spin filter (Millipore, Shanghai, China). Refolding of solubilized recombinant proteins by 8 to 2 mol/L urea gradient size-exclusion chromatography was performed on an XK 16/100 column packed with Superdex 75 gel media (GE Healthcare). The concentrated peak fractions were desalted on a 5 mL Bio-Gel P-6 desalting column (Bio-Rad, Shanghai, China). All procedures were carried out at 4 °C. The purified proteins were lyophilized and stored at −80 °C before use.

Antibody preparation and Western blot analysis

Antibody preparation was performed as reported previously (Ren et al., 2019). In brief, purified recombinant proteins, dissolved in PBS and emulsified with Freund's incomplete adjuvant, were used to immunize mice by intraperitoneal injection once every 7 d for a total of four injections. Control mice were injected with incomplete Freund's adjuvant. Whole blood was collected and centrifuged at 13 000 r/min for 15 min at 4 °C to obtain serum. Anti-PaFcγRIm, anti-PaIgM-Fc, and control isotype antisera were purified by protein G chromatography media (Bio-Rad). Antiserum quality was tested by Western blot analysis as described previously (Ren et al., 2019), and visualized using an enhanced chemiluminescence (ECL) kit (Advansta, Menlo Park, USA). The antiserum with 0.2% sodium azide was kept at −20 °C until use. For the determination of PaFcγRI glycosylation, PNGase F (New England Biolabs, Beverly, MA, USA) was used to digest kidney proteins followed by Western blot analysis.

The monocytes/macrophages (MO/MΦ), lymphocytes, and neutrophils were isolated and enriched as described below

(Chen et al., 2016, 2018). Ayu head kidney was aseptically extracted and pushed with a glass rod through a 100 μm wire mesh. The resultant single-cell suspension was layered onto Ficoll-Hypaque PREMIUM (1.077 g/mL) (GE Healthcare). After centrifugation at 400 g for 25 min at room temperature, the buffy layer above the Ficoll was collected and washed with RPMI 1640 medium (Invitrogen) supplemented with 2% fetal bovine serum (FBS; Invitrogen), penicillin (100 U/mL), streptomycin (100 U/mL), and heparin (20 U/mL). Cells were cultured for 12 h, with the attached cells identified as enriched MO/MΦ. Blood samples were collected and layered onto Ficoll-Hypaque PREMIUM (1.077 g/mL) at a density gradient, then centrifuged at room temperature for 25 min at 400 g. Neutrophils below the Ficoll (containing erythrocytes) were subjected to hypotonic lysis treatment with ice-cold ACK lysis buffer. The non-adherent lymphocytes were collected from the buffy layer by differential adherence to exclude MO/MΦ. PaFcγRI expression in tissues (liver, spleen, and kidney) and cells (MO/MΦ, lymphocytes, and neutrophils) was determined by Western blot analysis.

***In vitro* secretion**

To test whether the native leader of PaFcγRI could generate a secreted protein, PaFcγRI was amplified using the primers listed in Table 2. The amplified product was cloned into the pcDNA3.1 mammalian expression vector (Invitrogen) and then transiently transfected into HEK293 cells using FuGENE® 6 Transfection Reagent (Promega, Madison, USA). The HEK293 cells were grown at 37 °C in a humidified incubator in the presence of 5% CO_2. The complete medium for the HEK293 cells was Dulbecco's modified Eagle's medium supplemented with 10% FBS. After 24 h, the supernatants and cell lysates were examined for recombinant PaFcγRI (rPaFcγRI) (containing signal peptide) by Western blotting using the anti-PaFcγRIm antiserum. To further demonstrate the secretion characteristics of PaFcγRI, Western blotting was used to detect the native protein in ayu serum.

Interaction between PaFcγRI and ayu IgM (PaIgM) identified by flow cytometry

The interaction between two recombinant proteins was identified by flow cytometry, as described in Seijsing et al. (2013). Firstly, a recombinant TM protein, with mCherry on its N-terminal and PaIgM heavy chain on its C-terminal (mCherry-TM-PaIgM), was expressed on the HEK293 cell membrane. The TM-PaIgM fragment (111 bp+1 761 bp=1 872 bp) was obtained by overlap extension PCR. The primers for amplifying TM were designed according to the TM domain (aa 53–75) of the ayu C-type lectin receptor gene (Table 2). The control protein (mCherry-TM) was a recombinant TM protein with mCherry on the C-terminal. To construct the recombinant plasmids, amplicons of expected size were digested by *Bam*H I and *Eco*R I, and subsequently inserted into the pCMV-N-mCherry vector (Beyotime Biotechnology, Shanghai, China). The recombinant plasmid was then constructed and transfected into the HEK293 cell line by FuGENE® 6 Transfection Reagent. The expression of recombinant mCherry-TM-PaIgM and mCherry-TM were visualized using a Nikon Eclipse Ti-U fluorescence microscope. Their expression levels were also detected using anti-mCherry antibody by Western blot analysis.

The HEK293 cells expressing mCherry-TM-PaIgM or mCherry-TM were incubated with anti-PaIgM-Fc antiserum for 1 h at 37 °C. After washing, the cells were incubated with secondary antibody, FITC-labeled goat anti-mouse IgG (Beyotime Biotechnology), for 1 h at 37 °C. Finally, the cells were washed and analyzed by a Gallios flow cytometer (Beckman Coulter, California, USA).

The HEK293 cells expressing mCherry-TM-PaIgM or mCherry-TM were respectively incubated with rPaFcγRIm for 1 h at 37 °C, and then washed and incubated with anti-PaFcγRIm antiserum for 1 h at 37 °C. After this, the cells were washed and incubated with FITC-labeled goat anti-mouse IgG (Beyotime Biotechnology) for 1 h at 37 °C, then washed and resuspended in PBS supplemented with 1% bovine serum albumin (BSA). Cells were analyzed in a Gallios flow cytometer and 10 000 events per sample were recorded. The data were processed using Kaluza software (Beckman Coulter).

Primary anti-sheep red blood cell (SRBC) responses *in vitro*

The biological activity of rPaFcγRIm was tested on primary anti-SRBC responses *in vitro* using a modified hemolytic plaque-forming cell (PFC) assay (Jacobson et al., 2003; Kaattari et al., 1986; Smith, 1998; Varin et al., 1989). Anesthetized fish were sacrificed and placed on ice. The spleens were excised under sterile conditions and immediately placed into 2 mL of cold Hank's balanced salt solution (HBSS) (Sangon Biotech, Shanghai, China) in sterile plastic 2 cm petri dishes. Spleen cells were separated by gentle maceration over a 100 μm nylon screen, transferred to 15 mL conical tubes, and incubated with ACK Lysis Buffer (Beyotime Biotechnology) for 5 min at room temperature. The spleen cells were washed twice with cold HBSS and centrifuged at 2 000 r/min for 10 min at 4 °C. The resulting cellular pellet was resuspended in 2 mL cold complete media (RPMI 1640, 10% FBS, 100 U/mL penicillin, and 100 mg/mL streptomycin). A 50 μL aliquot was removed and combined with 450 μL of 10% trypan blue for lymphocyte differentiation, enumeration, and viability in a hemocytometer at 40×. Each sample was diluted to 8×10^6 cells per mL in complete media, after which 50 μL of 20% SRBCs per mL was added and the sample was cultured for 3 d at 24 °C and 5% CO_2. At day 3, purified rPaFcγRIm was added, which was serially diluted (1: 2) (original concentration 5 μg/mL) to a 100 μL final volume, with a sample without rPaFcγRIm used as the control. At day 5, each sample (250 μL) was combined with 0.15 mL of 20% SRBCs and 0.8 mL of 45 °C 0.7% agar solution, then mixed quickly and poured into 5 cm plastic petri dishes and allowed to solidify. Plates were incubated for 2 h with humidity at 24 °C to allow specific lymphocyte recognition of SRBCs and subsequent antibody production and binding. After this, 1 mL of 10% complement source serum (diluted by HBSS)

was added and the plates were incubated overnight at 24 °C to allow complement-mediated lysis of the SRBCs. Plaques were enumerated and evaluated for approximate size manually via a low-powered Guiguang XTL-400 dissecting microscope with 10× ocular strength. Inhibition >30% was considered significant in view of the variability of this technique.

RESULTS

Cloning and sequence analysis of PaFcγRI

The cDNA sequence of PaFcγRI was 1 113 nucleotides (nts) in length, comprising a 5'-UTR of 79 nts, 3'-UTR of 125 nts, and open reading frame of 909 nts, and encoding a polypeptide of 302 amino acids (aa) with a predicted molecular weight (MW) of 34.1 kDa. BLAST searching revealed that this sequence was homologous to mammalian FcγR and was thus tentatively named PaFcγRI. It was predicted to comprise of a signal peptide (aa 1−33) and two Ig domains: Ig domain 1 (D1) consisting of 80 aa (aa 43−122) and Ig domain 2 (D2) consisting of 85 aa (aa 130−214). Both Ig domains contained two conserved cysteine residues (Cys), essential for the formation of disulfide bonds (predicted as $Cys^{58}-Cys^{98}$ and $Cys^{145}-Cys^{191}$) (Figure 1). The two disulfide bonds were conserved in all selected mammalian and fish FcRs (Figure 1B). According to the features, such as the spacing of cysteine bridges and number of beta sheets, D1 and D2 were classified as C2 domains and shared homology with low-affinity receptor domains. Furthermore, PaFcγRI had three potential N-glycosylation sites: i.e., N^{112}NS, N^{177}LT, and N^{180}LT.

Sequence comparison analysis showed that PaFcγRI was tightly grouped with previously reported Nile tilapia (*Oreochromis niloticus*) (identity 35.4%) and Japanese ricefish (*Oryzias latipes*) (identity 34.4%), suggesting an evolutionary relationship. Phylogenetic tree analysis revealed that PaFcγRI fell into a larger cluster that included fish FcRs, and also grouped with the mammalian FcγR subset (Figure 2A). In addition, each PaFcγRI domain had a related counterpart that variously occurred throughout the FcγRs (Figure 2B).

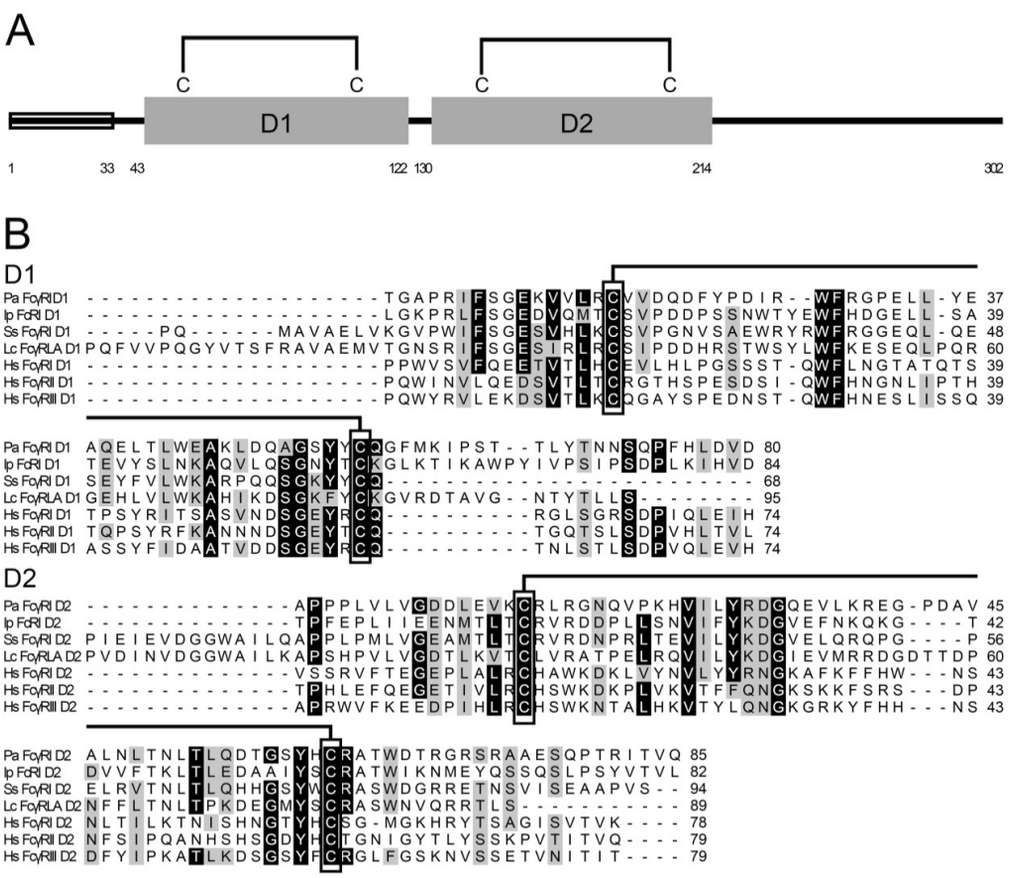

Figure 1 Schematic representation and multiple alignments of amino acid sequences

A: Schematic representation of PaFcγRI protein including signal peptide (box) and disulfide bonds (line). B: Amino acid alignments of D1 and D2 of ayu, channel catfish, Atlantic salmon, large yellow croaker, and representative human FcγRs. Hatched boxes indicate conserved cysteines and dashes (-) represent gaps. IpFcRI: Channel catfish FcRI; SsFcγRI: Atlantic salmon FcγRI; LcFcRLA: Large yellow croaker FcRLA; HsFcγRI: Human FcγRI; HsFcγRII: Human FcγRII; HsFcγRIII: Human FcγRIII. GenBank accession Nos. are listed in Table 1.

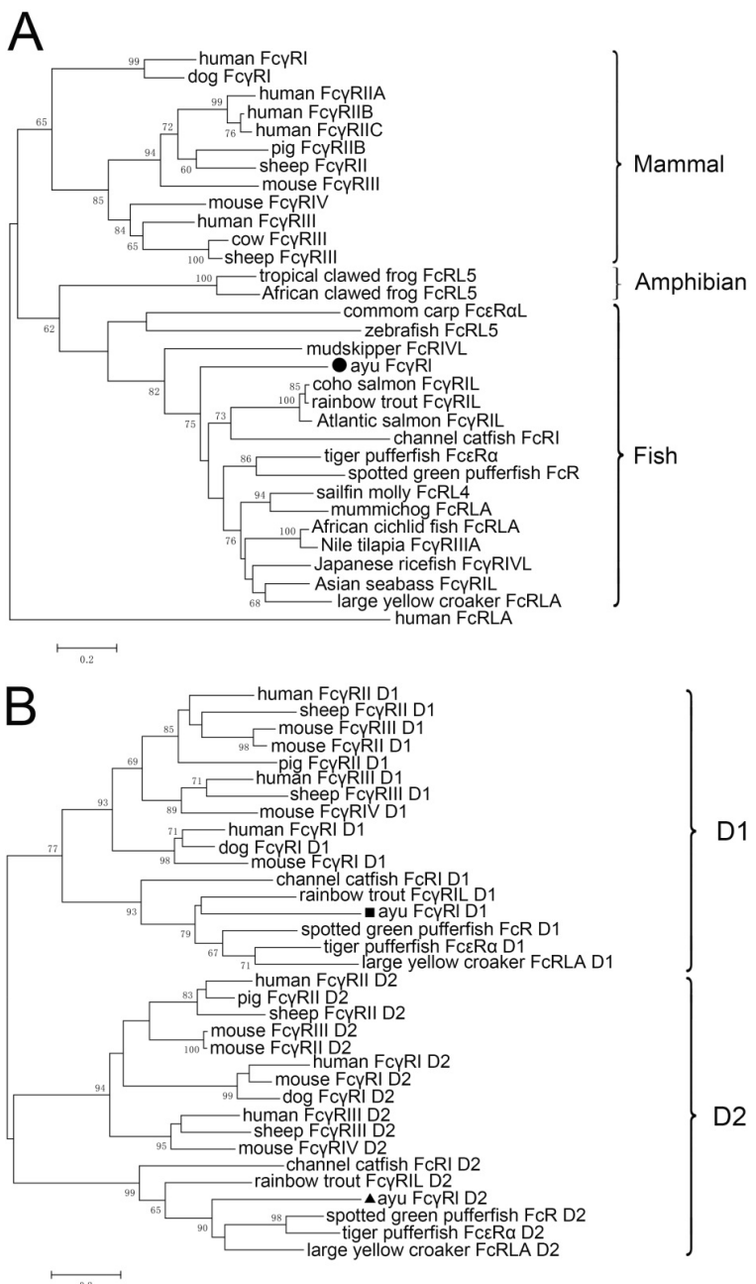

Figure 2 Phylogenetic analysis of full-length (A) and two Ig domain (B) amino acid sequences of PaFcγRI and related FcRs using neighbor-joining method

Values at forks indicate percentage of trees in which this grouping occurred after bootstrapping (1 000 replicates; shown only when >60%) using MEGA7.0. Scale bar shows number of substitutions per base.

Tissue expression profiles of PaFcγRI transcripts

PaFcγRI mRNA was expressed in the liver, spleen, kidney, brain, intestines, muscle, and gill at low levels, with the highest expression detected in the gill of healthy ayu (Figure 3A). Following *V. anguillarum* infection, PaFcγRI mRNA expression was up-regulated in all tested tissues (Figure 3B–E). After stimulation with viable *V. anguillarum*, the up-regulation of PaFcγRI expression in the liver and spleen demonstrated an inverted U-shaped tendency. The highest expression levels of PaFcγRI in the liver, spleen, and kidney were detected at 8 hpi and in the gill were detected at 4 hpi. Furthermore, PaFcγRI mRNA expression levels in the liver,

spleen, kidney, and gill were up-regulated by 19.30-fold, 16.05-fold, 19.01-fold, and 4.78-fold, respectively, after stimulation (Figure 3B–E).

Prokaryotic expression, purification, and antibody preparation of rPaFcγRIm and rPaIgM-Fc

After induction by IPTG, the recombinant proteins were all over-expressed in *E. coli* BL21 (DE3). The size of rPaFcγRIm on the 12% SDS-PAGE gel was ~40 kDa, similar to the calculated MW of 39.8kDa (34.1 kDa PaFcγRIm plus 5.7 kDa His-tag) (Figure 4A). The size of rPaIgM-Fc on the 12% SDS-PAGE gel was 44 kDa, similar to the calculated MW of 43.2 kDa (37.5 kDa rPaIgM-Fc plus 5.7 kDa His-tag) (Figure 4C). The purifications of the two recombinant proteins were all greater than 95%.

Western blot analysis revealed that the MW of native PaFcγRI in the ayu kidney was ~47 kDa and after deglycosylation was ~34 kDa, similar to sequence calculations (34.1 kDa) (Figure 4B). Western blot analysis also revealed that the MW of the native PaIgM heavy chains in ayu was ~ 70–80 kDa, similar to the MW of IgM heavy chains reported previously in fish (Wilson & Warr, 1992) (Figure 4D).

Furthermore, Western blot analysis revealed native protein expression in the healthy head kidney and trunk kidney, but not in the liver or spleen (Figure 4E). The detected cell types that expressed PaFcγRI were neutrophils, but not MO/MΦ or lymphocytes (Figure 4E).

***In vitro* secretion of rPaFcγRI**

Results showed rPaFcγRI with the native leader was expressed in the HEK293 cells. As shown in Figure 5A, rPaFcγRI was ~49 kDa (calculated MW 34.1 kDa), which might be caused by glycosylation, as expressed in HEK293 cells. rPaFcγRI was detected in both the supernatants and cell lysates of pcDNA3.1-PaFcγRI-transfected cells but not in the supernatants and cell lysates of the control cells transfected with pcDNA3.1, indicating that the native leader can indeed generate a secretory PaFcγRI. Native PaFcγRI in serum was also detected by Western blotting. In the sera of the healthy control and infected ayu, no obvious bands were observed at 4, 8, or 12 hpi, whereas an obvious band was observed in the infected ayu at 24 hpi (Figure 5B).

rPaFcγRIm binding to PaIgM

PaIgM was expressed as a fusion protein, which included PaIgM+TM+mCherry. Its expression was first detected in HEK293 cells by fluorescence microscopy. Results showed that mCherry was expressed in the cytoplasm, and the two recombinant proteins (mCherry-TM and mCherry-TM-PaIgM) were mainly localized on the plasma membrane (Figure 6A). Western blot analysis revealed that the MW of mCherry-TM was ~31 kDa, similar to the calculated MW of 30.5 kDa (3.8 kDa TM plus 26.7 kDa mCherry), and the MW of mCherry-TM-PaIgM was ~95 kDa, similar to the calculated MW of 95 kDa (68.3 kDa TM-PaIgM plus 26.7 kDa mCherry) (Figure 6B). Flow cytometry revealed that PaIgM was identified with anti-PaIgM-Fc antiserum, suggesting that the PaIgM part in mCherry-TM-PaIgM was mainly localized outside the HEK293 plasma membrane (Figure 6C). Finally, the interaction between rPaFcγRIm and the PaIgM Fc portion was detected by flow cytometry. Results showed that cells probed with FITC displayed a linear relationship between mCherry and FITC

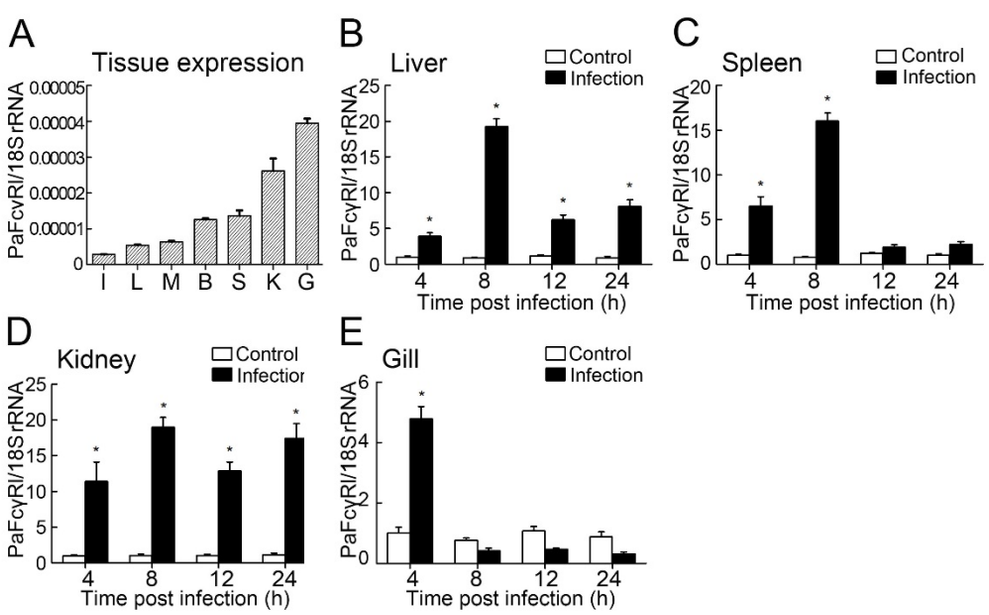

Figure 3 RT-qPCR detection of PaFcγRI expression in ayu tissues

A: Healthy tissues. L: Liver, S: Spleen, K: Kidney, B: Brain, G: Gill, I: Intestines, M: Muscle. B–E: PaFcγRI transcripts in ayu challenged with *V. anguillarum* infection. Tissues were collected at different time points post-infection. PaFcγRI transcript levels were normalized to Pa18S rRNA transcript levels. Data are means±*SEM* of the results from four fish. *: $P<0.05$.

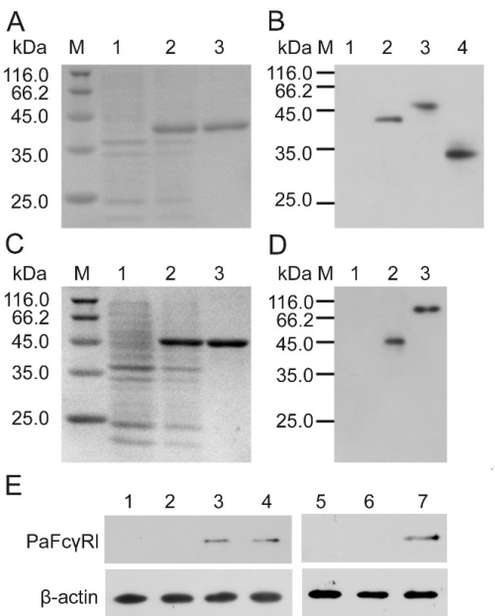

Figure 4 Prokaryotic expression and Western blot analysis

A: 12% SDS-PAGE analysis of bacterial lysates and purified rPaFcγRIm. Lane M: Protein marker; 1: pET30a-PaFcγRIm/BL21 before IPTG induction; 2: pET30a-PaFcγRIm/BL21 after IPTG induction; 3: Purified rPaFcγRIm. B: Western blot analysis of rPaFcγRIm using anti-PaFcγRIm antiserum. Lane M: Protein marker; 1: pET30a-PaFcγRIm/BL21 before IPTG induction; 2: pET30a-PaFcγRIm/BL21 after IPTG induction; 3: Ayu kidney lysates; 4: Ayu kidney lysates after deglycosylation by PNGase F. C: 12% SDS-PAGE analysis of bacterial lysates and purified rPaIgM-Fc. Lane M: Protein marker; 1: pET30a-PaIgM-Fc/BL21 before IPTG induction; 2: pET30a-PaIgM-Fc/BL21 after IPTG induction; 3: Purified rPaIgM-Fc. D: Western blot analysis of rPaIgM-Fc using anti-PaIgM-Fc antiserum. Lane M: Protein marker; 1: pET30a-PaIgM-Fc/BL21 before IPTG induction; 2: pET30a-PaIgM-Fc/BL21 after IPTG induction; 3: Ayu spleen lysates. E: Protein expression of PaFcγRI in different tissues and cell types. 1: Liver; 2: Spleen; 3: Head kidney; 4: Trunk kidney; 5: MO/MΦ, 6: Lymphocytes; 7: Neutrophils.

fluorescence, indicating a linear correlation between the amounts of mCherry-TM-PaIgM and binding of rPaFcγRIm (Figure 6D). The control (mCherry-TM and rPaFcγRIm) did not show such a correlation (Figure 6D).

Suppressive activity of rPaFcγRIm on *in vitro* IgM anti-SRBC antibody responses

The biological activity of rPaFcγRIm on primary anti-SRBC antibody responses *in vitro* was tested. As shown in Figure 7, rPaFcγRIm suppressed anti-SRBC antibody production in a dose-dependent fashion. About 1.70 μg/mL of rPaFcγRIm was necessary to inhibit 50% of antibody production against SRBCs. This effect was not due to toxicity, as the addition of rPaFcγRIm did not decrease viability of the spleen cells.

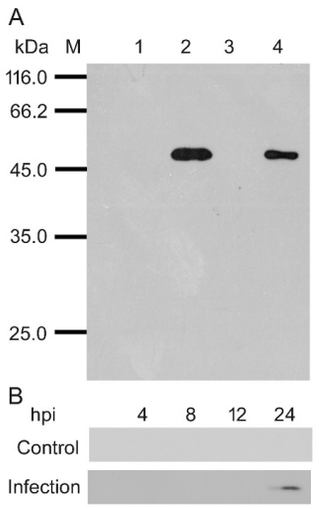

Figure 5 Secretion of rPaFcγRI

A: PaFcγRI was cloned into pcDNA3.1 and transiently transfected into HEK293 cells. After 24 h, supernatants and cell lysates were examined by Western blotting using anti-PaFcγRIm antiserum. Lane M: Protein marker; 1: Supernatants of pcDNA3.1/HEK293, negative control; 2: Supernatants of pcDNA3.1-PaFcγRI/HEK293; 3: Cell lysates of pcDNA3.1/HEK293, negative control; 4: Cell lysates of pcDNA3.1-PaFcγRI/HEK293. B: Native PaFcγRI in ayu serum.

DISCUSSION

Myeloid leukocytes in humans and mice are equipped with a variety of receptors that enable their interaction with monomeric or aggregated immunoglobulins, antigen-antibody immune complexes, and opsonized antibody-coated particles or cells (Pierre & Friederike, 2015). FcγRs are receptors that induce diverse biological functions after binding to the Fc portion of antibodies mediated by extracellular domains. The extracellular domains of mammalian FcγRI contain three Ig domains (i.e., D1, D2, and D3), whereas FcγRII, FcγRIII, and FcγRIV only contain the first two (i.e., D1 and D2). D1 and D2 are highly homologous among species, whereas D3 shows a lower level of homology, although it is still clearly related to the Ig superfamily (Sears et al., 1990). Interestingly, there is a group of teleost proteins closely homologous to the extracellular domains of mammalian FcγRs (Stafford et al., 2006). Among such homologous proteins, most contain two Ig domains (D1, D2), although a few contain three or four. For example, IpFcRI contains three Ig domains (D1, D2, and D3), with D1 and D2 found clustered with high bootstrap values with mammalian FcR Ig-domain counterparts, but D3 not phylogenetically related to any mammalian FcR Ig domain (Stafford et al., 2006). Likewise, there are a different number of Ig domains in the FcR sequences of zebrafish, rainbow trout, tiger puffer, and spotted green pufferfish (Akula et al., 2014; Stafford et al., 2006). Here, we studied an FcγR-like gene, PaFcγRI, from ayu. Phylogenetic tree analysis showed that PaFcγRI and other fish FcRs were grouped together and

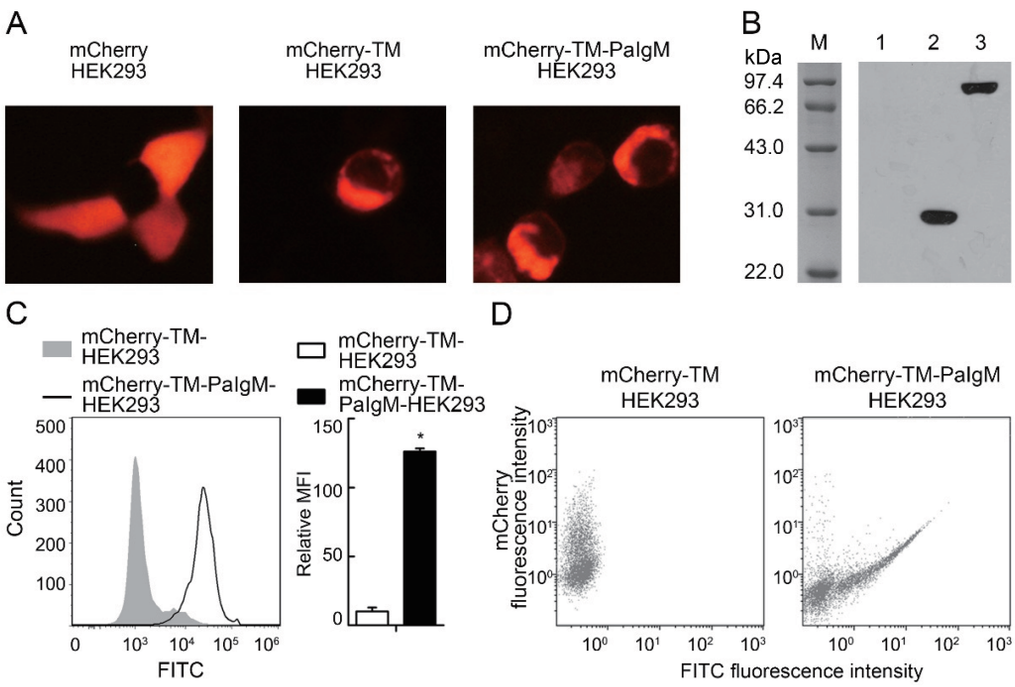

Figure 6 Interaction between rPaFcγRIm and PaIgM

A: Localization of mCherry, mCherry-TM, and mCherry-TM-PaIgM in HEK293 cells observed by fluorescence microscopy. B: Western blot analysis of mCherry-TM and mCherry-TM-PaIgM expression in HEK293 cells with anti-mCherry antibody. Lane M: Protein marker; 1: HEK293 cells, negative control; 2: mCherry-TM/HEK293; 3: mCherry-TM-PaIgM/HEK293. C: Flow cytometry analysis of percentage of HEK293 cells expressing mCherry-TM-PaIgM following incubation with anti-PaIgM-Fc antiserum. Histogram showing percentage of mCherry-TM-PaIgM-positive cells in mCherry-TM-PaIgM/HEK293 and mCherry-TM-PaIgM/HEK293 detected by flow cytometry analysis with anti-PaIgM-Fc antiserum. Data are means±*SEM* of results from four assays. *: $P<0.05$. D: Flow cytometry analysis of binding of rPaFcγRIm to PaIgM. HEK293 cells overexpressing mCherry-TM and mCherry-TM-PaIgM were first probed with rPaFcγRIm, then detected with anti-PaFcγRIm antiserum produced in mice and stained with FITC-labeled goat anti-mouse IgG.

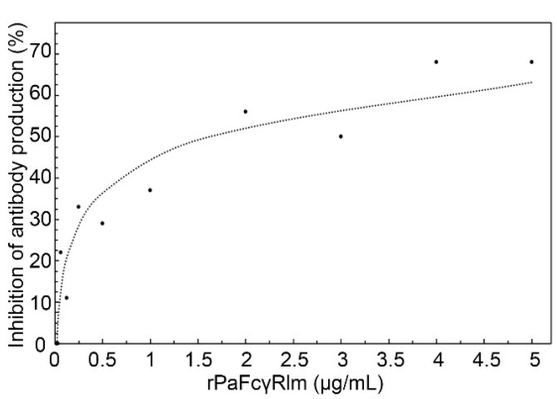

Figure 7 rPaFcγRIm inhibits anti-SRBC antibody production

Various doses of rPaFcγRIm were added at day 3 to cultures of spleen cells stimulated by SRBCs. Anti-SRBC antibody production was measured at day 5 by direct PFC assay.

were also clustered with the mammalian FcγR subset. In addition, PaFcγRI possessed only D1 and D2, which were classified into C2 sets and phylogenetically related to the corresponding domain of mammalian and fish FcγRs, respectively.

Tissue and cellular mRNA expression of the FcγR homolog has been studied in channel catfish. Stafford et al. (2006) readily detected IpFcRI transcripts by Northern blot analysis in the spleen and hemopoietic kidney tissues of channel catfish, as well as in their peripheral blood leukocytes (PBLs) (predominantly in granulocytes). To date, however, no information regarding mRNA expression of FcγR homologs related to infection has been reported. Mammalian sFcγRs have been detected in biological fluids of mice and humans, with production found to be highly dependent on environmental factors, including pathogens. For example, mouse sFcγRII (Fcγ2b/γ1R) was reported to increase in culture medium after stimulation of spleen cells with lipopolysaccharide (LPS), which was attributed to B lymphocytes (Pure et al., 1984). Furthermore, a dramatic increase in circulating sFcγRII is also found in *Schistosoma mansoni*-infected mice (Khayat et al., 1986). In the current study, PaFcγRI mRNA was expressed at low levels in all tested tissues, with the highest expression found in the gill. Furthermore, expression in the liver, spleen, and kidney showed sensitive responses to *V. anguillarum* infection. With antiserum, the PaFcγRI protein was also detected in the head

kidney, trunk kidney, and neutrophils.

The teleost proteins mentioned in this study are soluble, thus differing from the mammalian membrane-bound FcγRs. This suggests that this group of proteins may be secreted and/or intracellularly expressed, thus hinting at their function. In channel catfish, IpFcRI was identified as a secretory protein in the serum akin to sFcR found in mammals (Stafford et al., 2006). In this study, rPaFcγRI was also found to be secreted in the supernatants of HEK293 cells. Native PaFcγRI was also detectable in serum challenged with *V. anguillarum*.

The binding of the Fc region of IgG to FcγR is a critical step for the initiation and control of effector immune functions (Sibéril et al., 2007). For the IgG ligands, FcγRI and FcγRIV are high-affinity receptors, whereas FcγRII and FcγRIII are low-affinity receptors (Qiu et al., 1990). Mouse and human sFcγRs bind to IgG subclasses with a binding profile identical to the corresponding membrane-associated receptors and exhibit immunomodulatory properties (Lynch et al., 1992). In fish, only IpFcRI has been identified to bind with IgM, as assessed by co-immunoprecipitation and cell transfection studies (Stafford et al., 2006). In our research, rPaFcγRIm was found to bind with IgM, which might provide a hint to its function in immunity.

As reported earlier, mammalian sFcγRs inhibit *in vitro* and *in vivo* immune responses. For instance, purified mouse sFcγRIIB1 exerts dose-dependent suppressive activity on primary and secondary antibody responses when added to cultures of spleen cells stimulated with SRBCs, with the effect even more pronounced on IgG than on IgM responses (Varin et al., 1989). Sautès et al. (1992) also found that sFcγRIIB1 inhibits antibody *in vitro* responses to SRBCs in small B cell cultures stimulated by anti-IgM antibodies in the presence of IL-4 and IL-5. Moreover, intraperitoneal injection of this material into adult mice immunized with SRBCs decreases IgG antibody production in spleen cells, as measured by PFC assay, and in serum, as measured by antigen-specific ELISA (Sautès et al., 1992). Furthermore, purified human sFcγRIIIB (sCD16) inhibits IgM and IgG production of human peripheral blood mononuclear cells stimulated by pokeweed mitogen *in vitro* in a time and dose-dependent manner (Teillaud et al., 1993). sFcγRs are believed to function by competing with their membrane-bound counterparts for Ig (or immune complex) binding, which, in turn, down-regulates B cell proliferation and antibody production (Fridman et al., 1993). In our study, the PaFcγRI protein was not detectable in the serum of healthy ayu but was up-regulated upon infection. We identified that rPaFcγRIm exerts suppressive activity on primary antibody responses *in vitro* at a relatively high concentration. Thus, we speculated that PaFcγRI might be involved in the down-regulation of antibody levels at the late stage of infection.

In summary, we showed that PaFcγRI exhibited sequence characteristics similar to classical FcRs with extracellular domains. Furthermore, we revealed that PaFcγRI was a secretory protein bound to PaIgM. *In vitro*, PaFcγRI likely plays a role in the regulation of IgM production.

COMPETING INTERESTS

The authors declare that they have no competing interests.

AUTHORS' CONTRIBUTIONS

Y.H.S. and J.C. drafted the experiments; K.C. and Y.H.S. performed the experiments; K.C., Y.H.S., J.C., and M.Y.L. analyzed the data and wrote the paper. All authors read and approved the final version of the manuscript.

REFERENCES

Akula S, Mohammadamin S, Hellman L. 2014. Fc receptors for immunoglobulins and their appearance during vertebrate evolution. *PLoS One*, **9**(5): e96903.

Bournazos S, Ravetch JV. 2015. Fcγ receptor pathways during active and passive immunization. *Immunological Reviews*, **268**(1): 88–103.

Chen F, Lu XJ, Nie L, Ning YJ, Chen J. 2018. Molecular characterization of a CC motif chemokine 19-like gene in ayu (*Plecoglossus altivelis*) and its role in leukocyte trafficking. *Fish & Shellfish Immunology*, **72**: 301–308.

Chen Q, Lu XJ, Li MY, Chen J. 2016. Molecular cloning, pathologically-correlated expression and functional characterization of the colonystimulating factor 1 receptor (CSF-1R) gene from a teleost, *Plecoglossus altivelis*. *Zoological Research*, **37**(2): 96–102.

Daëron M, Sautès C, Bonnerot C, Blank U, Varin N, Even J, Hogarth PM, Fridman WH. 1989. Murine type II Fc gamma receptors and IgG-binding factors. *Chemical Immunology*, **47**: 21–78.

Davis RS. 2007. Fc receptor-like molecules. *Annual Review of Immunology*, **25**: 525–560.

Davis RS, Ehrhardt GRA, Leu CM, Hirano M, Cooper MD. 2005. An extended family of Fc receptor relatives. *European Journal of Immunology*, **35**(3): 674–680.

DiLillo DJ, Ravetch JV. 2015. Fc-receptor interactions regulate both cytotoxic and immunomodulatory therapeutic antibody effector functions. *Cancer Immunology Research*, **3**(7): 704–713.

Esposito-Farese ME, Sautès C, de la Salle H, Latour S, Bieber T, de la Salle C, Ohlmann P, Fridman WH, Cazenave JP, Teillaud JL. 1995. Membrane and soluble Fc gamma RII/III modulate the antigen-presenting capacity of murine dendritic epidermal Langerhans cells for IgG-complexed antigens. *The Journal of Immunology*, **155**(4): 1725–1736.

Fridman WH, Bonnerot C, Daeron M, Amigorena S, Teillaud JL, Sautes C. 1992. Structural bases of Fcγ receptor functions. *Immunological Reviews*, **125**(1): 49–76.

Fridman WH, Teillaud JL, Bouchard C, Teillaud C, Astier A, Tartour E, Galon J, Mathiot C, Sautes C. 1993. Soluble Fc gamma receptors. *Journal of Leukocyte Biology*, **54**(5): 504–512.

Gavin AL, Wines BD, Powell MS, Hogarth PM. 1995. Recombinant soluble Fc gamma RII inhibits immune complex precipitation. *Clinical & Experimental Immunology*, **102**(3): 620–625.

Jacobson KC, Arkoosh MR, Kagley AN, Clemons ER, Collier TK, Casillas E. 2003. Cumulative effects of natural and anthropogenic stress on immune function and disease resistance in juvenile Chinook Salmon. *Journal of Aquatic Animal Health*, **15**(1): 1–12.

Kaattari SL, Irwin MJ, Yui MA, Tripp RA, Parkins JS. 1986. Primary *in vitro* stimulation of antibody production by rainbow trout lymphocytes. *Veterinary*

Immunology and Immunopathology, **12**(1–4): 29–38.

Khayat D, Serban D, Dux Z, Schlomo Y, Jacquillat C. 1986. Role of infection in the modulation of mouse circulating soluble cell-free Fcγ2b/γ1 receptor. *Scandinavian Journal of Immunology*, **24**(1): 83–91.

Kumar S, Stecher G, Tamura K. 2016. MEGA7: molecular evolutionary genetics analysis version 7.0 for bigger datasets. *Molecular Biology and Evolution*, **33**(7): 1870–1874.

Li CH, Chen J, Shi YH, Li MY. 2009. Characterization of *Listonella anguillarum* as the aetiological agent of vibriosis occurred in cultured ayu (*Plecoglossus altivelis*) in Ninghai country, China. *Acta Microbiologica Sinica*, **49**(7): 931–937.

Livak KJ, Schmittgen TD. 2001. Analysis of relative gene expression data using real-time quantitative PCR and the $2^{-\Delta\Delta CT}$ method. *Methods*, **25**(4): 402–408.

Lynch A, Tartour E, Teillaud JL, Asselain B, Fridman WH, Sautès C. 1992. Increased levels of soluble low-affinity Fcγ receptors (IgG-binding factors) in the sera of tumour-bearing mice. *Clinical & Experimental Immunology*, **87**(2): 208–214.

Matt P, Lindqvist U, Kleinau S. 2015. Elevated membrane and soluble cd64: a novel marker reflecting altered fcγr function and disease in early rheumatoid arthritis that can be regulated by anti-rheumatic treatment. *PLoS One*, **10**(9): e0137474.

Molenaar JL, Van Galen M, Hannema AJ, Zeijlemaker W, Pondman KW. 1977. Spontaneous release of Fc receptor-like material from human lymphoblastoid cell lines. *European Journal of Immunology*, **7**(4): 230–236.

Nayak DK, Tang A, Wilson M, Miller NW, Bengtén E. 2010. Channel catfish soluble FcμR binds conserved linear epitopes present on Cμ3 and Cμ4. *Molecular immunology*, **47**(6): 1306–1316.

Nishimori E, Kita-Tsukamoto K, Wakabayashi H. 2000. *Pseudomonas plecoglossicida* sp. *nov., the causative agent of bacterial haemorrhagic ascites of ayu, Plecoglossus altivelis. International Journal of Systematic and Evolutionary Microbiology*, **50**(1): 83–89.

Pierre B, Friederike J. 2015. Mouse and human FcR effector functions. *Immunological Reviews*, **268**(1): 25–51.

Puré E, Durie CJ, Summerill CK, Unkeless JC. 1984. Identification of soluble Fc receptors in mouse serum and the conditioned medium of stimulated B cells. *Journal of Experimental Medicine*, **160**(6): 1836–1849.

Qiu WQ, de Bruin D, Brownstein BH, Pearse R, Ravetch JV. 1990. Organization of the human and mouse low-affinity FcγR genes: duplication and recombination. *Science*, **248**(4956): 732–735.

Ren Y, Liu SF, Nie L, Cai SY, Chen J. 2019. Involvement of ayu NOD2 in NF-κB and MAPK signaling pathways: Insights into functional conservation of NOD2 in antibacterial innate immunity. *Zoological Research*, **40**(2): 77–88.

Rosales C, Uribe-Querol E. 2013. Antibody-Fc receptor interactions in antimicrobial functions. *Current Immunology Reviews*, **9**(1): 44–55.

Sarfati M, Chevret S, Chastang C, Biron G, Stryckmans P, Delespesse G, Binet JL, Merle-Beral H, Bron D. 1996. Prognostic importance of serum soluble CD23 level in chronic lymphocytic leukemia. *Blood*, **88**(11): 4259–4264.

Sautès C, Mazières N, Galinha A, Tartour E, Bonnerot C, Amigorena S, Teillaud C, Spagnoli R, Fridman WH. 1992. Murine soluble Fcγ receptors/IgG-binding factors (IgG-BF): Analysis of the relation to FcγRII and production of milligram quantities of biologically active recombinant IgG-BF. *Immunologic Research*, **11**(3–4): 181–190.

Sears DW, Osman N, Tate B, McKenzie IF, Hogarth PM. 1990. Molecular cloning and expression of the mouse high affinity Fc receptor for IgG. *The Journal of Immunology*, **144**(1): 371–378.

Seijsing J, Lindborg M, Löfblom J, Uhlén M, Gräslund T. 2013. Robust expression of the human neonatal Fc receptor in a truncated soluble form and as a full-length membrane-bound protein in fusion with eGFP. *PLoS One*, **8**(11): e81350.

Sibéril S, Dutertre CA, Fridman WH, Teillaud JL. 2007. FcγR: The key to optimize therapeutic antibodies?. *Critical Reviews in Oncology/Hematology*, **62**(1): 26–33.

Smith DA. 1998. The Development and Application of A Hemolytic Plaque Forming Cell Assay (PFC) and A Cytotoxic T-Lymphocyte Assay (CTL) in Tilapia (*Oreochromis niloticus*) for Immunotoxicity Risk Assessment of Environmental Contaminants. Ph.D. dissertation, Virginia Tech, 88–108.

Stafford JL, Wilson M, Nayak D, Quiniou SM, Clem LW, Miller NW, Bengtén E. 2006. Identification and characterization of a FcR homolog in an ectothermic vertebrate, the channel catfish (*Ictalurus punctatus*). *The Journal of Immunology*, **177**(4): 2505–2517.

Teillaud C, Galon J, Zilber MT, Mazières N, Spagnoli R, Kurrle R, Fridman WH, Sautès C. 1993. Soluble CD16 binds peripheral blood mononuclear cells and inhibits pokeweed-mitogen-induced responses. *Blood*, **82**(10): 3081–3090.

Tian J, Sun B, Luo Y, Zhang Y, Nie P. 2009. Distribution of IgM, IgD and IgZ in mandarin fish, *Siniperca chuatsi* lymphoid tissues and their transcriptional changes after *Flavobacterium columnare* stimulation. *Aquaculture*, **288** (1–2): 14–21.

van der Boog PJM, van Zandbergen G, de Fijter JW, Klar-Mohamad N, van Seggelen A, Brandtzaeg P, Daha MR, van Kooten C. 2002. FcαRI/CD89 circulates in human serum covalently linked to IgA in a polymeric state. *The Journal of Immunology*, **168**(3): 1252–1258.

Varin N, Sautès C, Galinha A, Even J, Hogarth PM, Fridman WH. 1989. Recombinant soluble receptors for the Fcγ portion inhibit antibody production *in vitro*. *European Journal of Immunology*, **19**(12): 2263–2268.

Wilson MR, Warr GW. 1992. Fish immunoglobulins and the genes that encode them. *Annual Review of Fish Diseases*, **2**: 201–221.

Xiong JB, Nie L, Chen J. 2019. Current understanding on the roles of gut microbiota in fish disease and immunity. *Zoological Research*, **40**(2): 70−76.

Zhang RC, Chen J, Li CH, Lu XJ, Shi YH. 2011. Prokaryotic expression, purification, and refolding of leukocyte cell-derived chemotaxin 2 and its effect on gene expression of head kidney-derived macrophages of a teleost fish, ayu (*Plecoglossus altivelis*). *Fish & Shellfish Immunology*, **31**(6): 911–918.